

# Young Galactic Globular Clusters II. The case of Pal 12. <sup>\*</sup>

A. Rosenberg<sup>1</sup>, I. Saviane<sup>2</sup>, G. Piotto<sup>2</sup>, and E.V. Held<sup>3</sup>

<sup>1</sup> Telescopio Nazionale Galileo, vicolo dell'Osservatorio 5, I-35122 Padova, Italy

<sup>2</sup> Dipartimento di Astronomia, Univ. di Padova, vicolo dell'Osservatorio 5, I-35122 Padova, Italy

<sup>3</sup> Osservatorio Astronomico di Padova, vicolo dell'Osservatorio 5, I-35122 Padova, Italy

**Abstract.** We present broadband  $V,I$  CCD photometry for  $\sim 1700$  stars towards the Galactic globular cluster Palomar 12, covering a field of  $10'.7 \times 10'.7$ . From these data, a color-magnitude diagram from the red giant branch tip to  $\sim 2$  mag below the cluster's turn-off is obtained. From a comparison with the color magnitude diagrams of 47 Tuc and M5, and using different theoretical models, we confirm that Pal 12 is younger, finding an age  $68 \pm 10\%$  that of both template clusters. Revised structural parameters are also obtained:  $r_c = 37.8 \pm 0.6$  and  $c = 1.08 \pm 0.02$ .

**Key words:** Hertzsprung-Russell (HR) diagram – stars: Population II – globular clusters: individual: Palomar 12

## 1. Introduction

The formation of the Galactic halo is presently at the center of an open debate. Stetson et al. (1996) state that, apart from a handful of anomalous clusters that may well have been captured from a satellite dwarf galaxy, there is no strong evidence for a significant spread in age among clusters of a given metal abundance, while Chaboyer et al. (1996) support an age spread of 5 Gyr among the bulk of the Galactic globular clusters (GGCs) (which is increased to 9 Gyr, if the youngest clusters are considered).

One of the largest underlying sources of uncertainty is the heterogeneity of the data used in these studies, which prevents “large scale” tests. This is the main reason that prompted our group to gather an homogeneous photometric data base of GGC, in  $V$  and  $I$ , as discussed in Saviane et al. (1997). To date, we have observed about 80% of the closest GGC's ( $(m - M)_v < 16$ ) with 1m class telescopes, and our data set allows us to obtain color-magnitude diagrams (CMDs) from the RGB tip down to a few magnitudes below the turn-off (TO).

Several young (or suspect young) GGCs were included in our program: Palomar 12 (Gratton & Ortolani 1988,

hereafter GO88), Ruprecht 106 (Buonanno et al.1990), Arp 2 (Buonanno et al. 1995a), Terzan 7 (Buonanno et al. 1995b) and Palomar 1 (Rosenberg et al. 1998, hereafter Paper I). Their age is suspected to significantly deviate from the general distribution. A precise determination of this deviation within our homogeneous data set is particularly valuable in the general framework of the GGC ages and of great importance in order to decide on the models of Galactic formation. For this reason, we will present and discuss in separate papers of this series the photometric data for the clusters whose age is significantly different from the average age of the GGC in our sample.

In Paper I we have discussed the case of Palomar 1, which resulted to be the youngest GGC in our Galaxy. In this paper we concentrate on Pal 12 (C2143-214,  $\alpha_{2000} = 21^h 46^m 6$ ,  $\delta_{2000} = -21^\circ 15'$ ;  $l = 30^\circ 5$ ,  $b = -47^\circ 7$ ) discovered by Harrington & Zwicky (1953) on the Palomar Sky Survey plates. Indeed, Pal 12 has been the first cluster to be classified as younger than the bulk of GGCs. However, the age determination in previous studies of its CMD, namely Stetson et al. (1989, hereafter S89), and Da Costa & Armandroff (1990, hereafter DA90) was affected by large uncertainties in its metal content (more than 0.3 dex in  $[\text{Fe}/\text{H}]$ ). Since then, new low- and high-resolution spectroscopy have been used in order to estimate the metallicity of Palomar 12 (Armandroff & Da Costa 1991, AD91; Brown et al. 1997, B97).

The observations and data reduction are presented in Sect. 2 and the resulting CMD is discussed in Sect. 3. The relative age determination is carried out in Sect. 4, and in Sect. 5 the structural parameters of the cluster are established.

## 2. Observations and data reductions

The data were collected on October 20, 1997 at the ESO Danish 1.54m telescope equipped with DFOSC. The camera employed a  $2048 \times 2048$  pixels Loral CCD, with a pixel size of  $0''.40$  on the sky, for a total field of view of  $13'.6 \times 13'.6$ .

*Send offprint requests to:* A. Rosenberg; alf@obelix.pd.astro.it

<sup>\*</sup> Based on data collected at the European Southern Observatory, La Silla, Chile

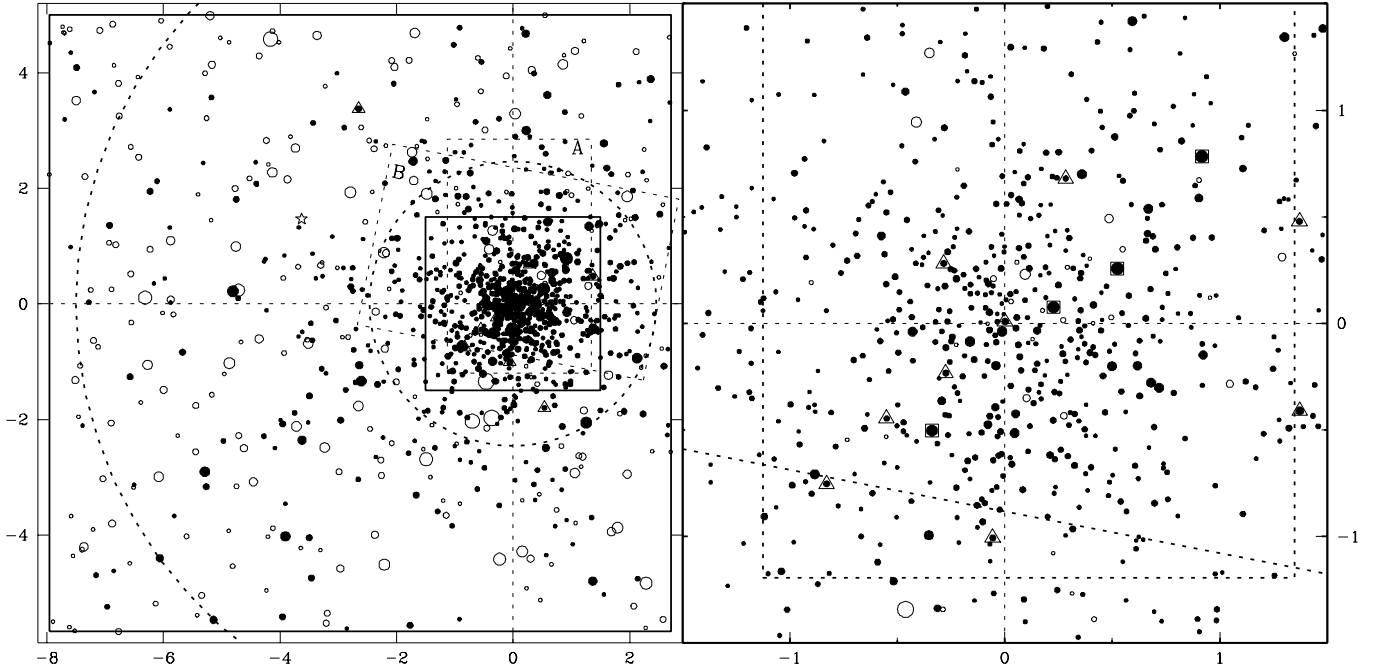


**Fig. 1.** Schematic representation of the complete ( $10'.7 \times 10'.7$ , *left*), and the central ( $1'.5 \times 1'.5$ , *right*) field, where stars brighter than  $V \sim 22.5$  are plotted. Coordinates are in arcmin (North is at the top, West to the right). Filled circles represent the stars within  $3\sigma$  in color from the fiducial sequence of the CMD plus BSS, HB and blended stars (see text for a detailed explanation). BSS are also marked as triangles, while squares indicate the stars for which spectroscopy has been obtained. Also, fields covered by GO88 (A) and S89 (B) are indicated (dashed rectangles). The tidal radius obtained by Trager et al, 1995 ( $2'.46$ ) is represented together with our new estimate based on the present data. A spiral galaxy is also clearly identified in our field, marked with a five-pointed star

**Table 1.** Journal of the Pal 12 observations for Oct 20, 1995

ID	Filter	$t_{\text{exp}}$ (s)	X	FWHM''
V1	V	20	1.010	0.9
V2	V	20	1.012	1.0
V3	V	40	1.013	1.0
V4	V	50	1.015	1.0
V5	V	50	1.016	1.0
V6	V	300	1.032	1.1
V7	V	300	1.040	1.1
I1	I	30	1.091	1.0
I2	I	40	1.086	1.0
I3	I	40	1.082	0.9
I4	I	40	1.074	0.9
I5	I	300	1.057	1.0
I6	I	300	1.049	1.0

Tab. 1 lists the complete log of the observations. The weather conditions were good during the night, which was stable and photometric, and the seeing was  $\sim 1''$ .

The image processing was carried out within the IRAF environment. First, a map of the bad features of the chip was created and they were removed from the raw images. Then, the bias stability was checked by comparing frames

taken at different times during the entire run, and no significant discrepancies were found. A 0.4 % spatial gradient was found along the  $x$  direction, thus a master bias image was created by taking the median of all the bias images. This master bias image was subtracted from all the remaining frames.

Sky flats were used to create master flat fields as medians of the single frames.

In order to avoid the fall of quantum efficiency (QE) all around the border of the Loral CCD, we cut our images outside the limit where the QE was 90% of the central value. From an inspection of the flats this limit imposed an effective area of  $1600 \times 1600$  pixels (i.e.  $10'.7 \times 10'.7$ ; Saviane & Held 1998, hereafter SH98, give further details). The effective field is schematically represented in Fig. 1.

Stellar photometry was performed using DAOPHOT, ALLSTAR (Stetson, 1987), and ALLFRAME, according to a standard procedure (see Paper I).

Observations of Landolt's (1992) standard stars were used to calibrate the photometry. In addition, the shutter delay time was measured with a sequence of images taken with increasing exposure times. A value of  $-0.11 \pm 0.01$ s (where the error is the standard deviation) was found.

The raw magnitudes were first normalized according to the following equation

$$m' = m_{\text{ap}} + 2.5 \log(t_{\text{exp}} + \Delta t) - k_{\lambda} X \quad (1)$$

where  $m_{\text{ap}}$  are the instrumental magnitudes measured in a circular aperture of radius  $R = 6''.9$  (SH98),  $\Delta t$  is the shutter delay and  $X$  is the airmass. For the extinction coefficients we adopted  $k_V = 0.135$  and  $k_I = 0.048$  (from the Geneva Observatory Photometric Group data).

The normalized instrumental magnitudes were then compared to the Landolt's (1992) values, and the following relations were found:

$$V = v' + 0.049(\pm 0.001)(V - I) + 23.766 \quad (2)$$

$$I = i' - 0.007(\pm 0.001)(V - I) + 23.070 \quad (3)$$

where the uncertainties represent the 90% confidence ranges of the fit for one interesting parameter. The standard deviations of the residuals are 0.013 mag in V and 0.022 mag in I, respectively.

In order to transform the PSF magnitudes into aperture magnitudes we assumed that  $m_{\text{ap}} = m_{\text{PSF}} + \text{const.}$  (Stetson 1987). For each individual frame a sample of bright isolated objects were then found, and all their neighbors were subtracted. The 'cleaned' images were used to measure aperture magnitudes for the selected stars, and for each star we computed the difference with respect to the PSF magnitude obtained on the averaged frames. The same aperture used for the standard stars was employed. The internal uncertainty of the calibration of the order of 0.01 mag for each filter (cf. SH98).

Our photometric catalogs are compared with those of Harris & Canterna 1980 (HC80), GO88, S89 and DA90 in Fig. 2. Noticeable differences are found for the V band, where a  $\Delta V \simeq 0.05$  mag is present between our values and those of HC80, S89 and DA90, in the sense that our magnitudes are fainter, and an even larger difference is found between our data and GO88 ( $\Delta V \simeq 0.12$  mag, cf Fig. 2). For the I band, only the DA90 data allow a comparison, and we find that the two calibrations match within the errors.

We tried to sort out the possible reason for the observed discrepancies in the V band, while no significant differences are found for the I band. From a comparison with existing photometry of the Fornax dwarf galaxy, SH98 conclude that their V band calibration is consistent with the previous works. A possible source of uncertainty could be a problem with the V exposure times: however, the (small) shutter delay has been included in Equation 1. Moreover, when the individual zero points of the 7 available V frames are compared, no differences larger than 0.01 mag are found, which furtherly confirms that there is no shutter delay problem. In principle, thin cirrus could have been present at the beginning of the night, although it should have blocked a remarkably constant percentage

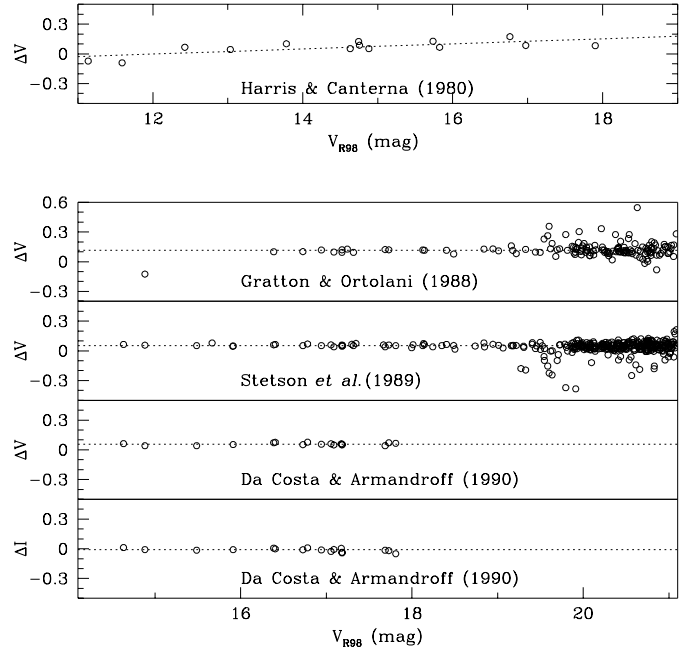


**Fig. 2.** Comparison with previous photometries. *Upper panel.* Differences in V between our data and HC80. *Lower panels.* Comparison with more recent CCD data. The mean difference between our data, GO88 and S89 is found to be  $\Delta V = 0.12 \pm 0.01$  mag and  $\Delta V = 0.05 \pm 0.01$  mag, respectively. The mean magnitude differences between our data and DA91 are  $\Delta V = 0.06 \pm 0.01$  mag and  $\Delta I = -0.01 \pm 0.01$ .

of light during the  $\sim 40$  min time span of the cluster observations, which seems unlikely. The above arguments lead us to trust our calibration, although further checks are needed in order to settle this issue.

In any case, the global zero-point difference in V between our Pal 12 photometry and that of the previous works will not affect our conclusions on the relative age of this cluster.

### 3. The Color-Magnitude Diagram

Fig. 3 shows the CMDs for the stars located inside (*left panel*) and outside (*right panel*) the known tidal radius ( $r_t \simeq 2''.5$ , Trager et al. 1995). The main features of the CMD can be clearly identified also in the outer region, implying either that the tidal radius must be larger than previous estimates (cf. Sect. 5 for a detailed discussion), or that Pal 12 is surrounded by a remarkable halo of extra-tidal radius cluster stars (Grillmair et al. 1995, Zaggia et al. 1997).

Stars from  $\sim 2$  mag below the turnoff (TO) up to the red giant branch (RGB) tip have been measured. Eleven blue straggler stars (BSS) are clearly identified in the region  $0.2 < V - I < 0.6$ ,  $18.2 < V < 20.2$ . Nine of them were already known, while two BSS are located outside the

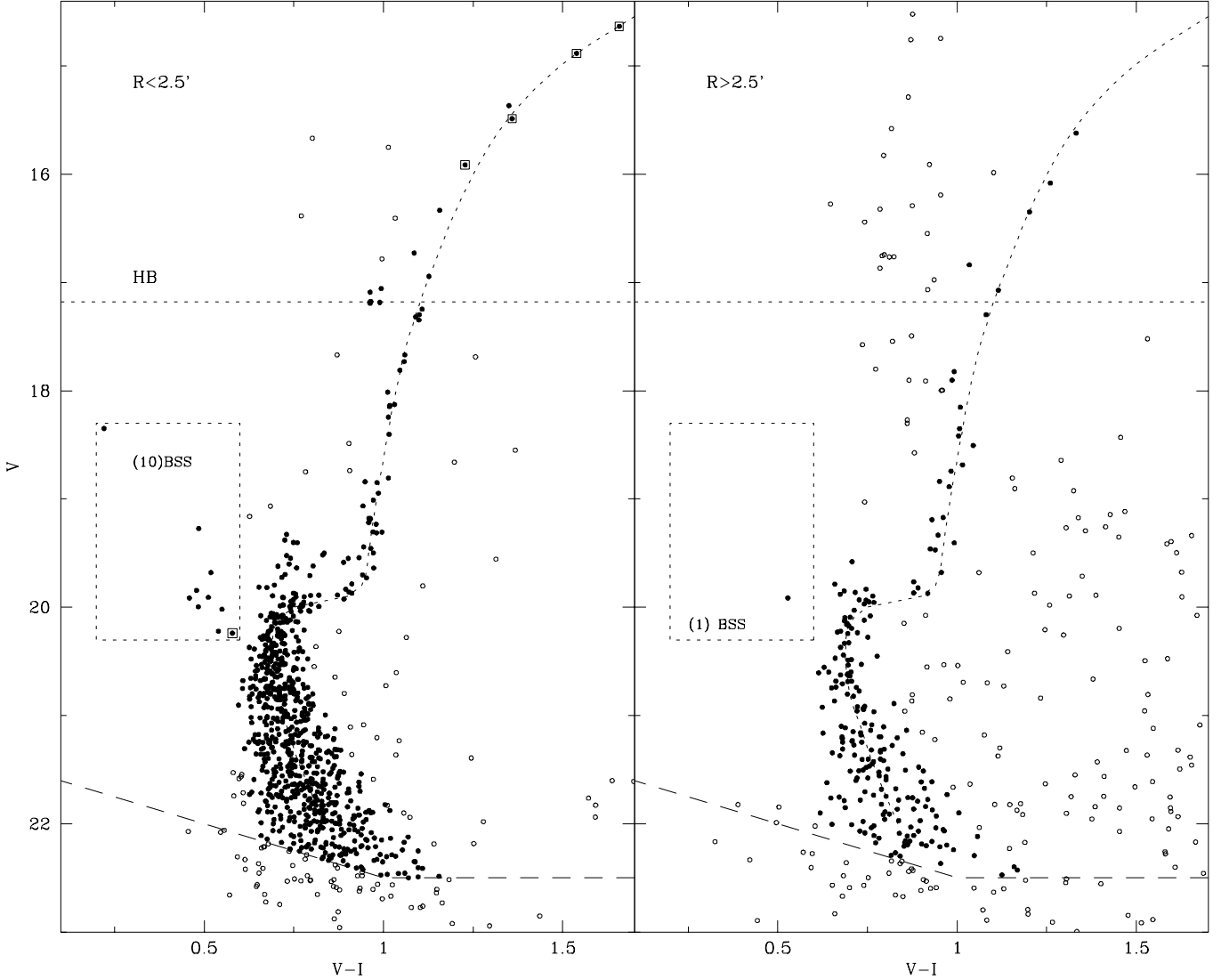


**Fig. 3.** Color-magnitude diagram for the inner ( $R < 2.5'$ , left panel), and the outer region (right panel) of Palomar 12. The adopted fiducial points are shown, together with the BSS region. The HB level is identified by a horizontal dotted line. The stars used for the computation of the cluster's profile are marked by filled circles. The 50% completeness level is represented by the dashed line. The four bright stars in the diagram, marked by squares, are those for which spectroscopy has been done (DA91, B97).

limits of the previously studied fields of the cluster. The BSS are marked with open triangles in Fig. 1. As shown in Fig 4, the BSS are more concentrated than the sub giant branch (SGB) stars with similar magnitude. This is consistent with what found in other GGCs, though the small number of BSS does not allow to assess the statistical significance of this result.

In the region  $0.60 < V - I < 0.85$  and  $18 < V < 19.8$  of the inner CMD a number of stars are present just above the TO. We have compared these stars with the corresponding objects in the S89 photometry. From this analysis we found that 45% of our objects are blends of 2 S89 stars, 20% are blends of 3 S89 stars and 35% of them are single stars in the S89 photometry (where the pixel

size is just  $0''.22$ , i.e. half of ours). Notice that almost no such stars are present in the outer, less crowded, region. It is likely that all stars with  $V < 20$  in Fig. 2 being significantly brighter in our photometry are photometric blends.

The horizontal branch (HB) is formed by 5 stars (already identified in the literature), and it is located in a very small region around the point  $(V - I, V) = (0.97, 17.18)$ , on the red side of the instability strip, as expected on the basis of the cluster metallicity. A dashed horizontal line marks the level of the HB in Fig. 3. The TO can be identified at  $(V - I) = 0.69 \pm 0.01$  and  $V = 20.50 \pm 0.1$ .

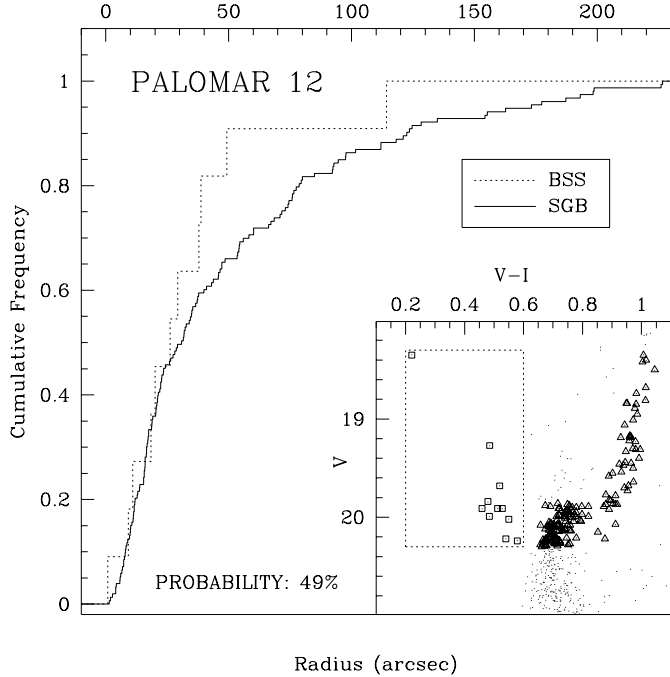


**Fig. 4.** Cumulative distribution of the BSS and the SGB stars with similar  $V$  magnitude in Pal 12. Though the BSS seem to be more concentrated than the SGB stars, their small number does not allow to assess the significance of this result. There is a probability of 49% for the null hypothesis that the two samples share the same radial distribution.

The foreground/background star contamination is low, as expected from the high galactic latitude of the cluster ( $b \simeq -48^\circ$ ). This is clearly seen by comparing the right and left panels of Fig. 3; the right panel shows the typical pattern of the halo background, superposed to the cluster CMD. The field contamination is redder than the Pal 12 MS, and decreases from fainter to brighter magnitudes. Notice also that the central CMD area is 5 times smaller than the external one, so that the cluster/background ratio clearly favors Pal 12 stars.

In order to determine the cluster profile, we defined a sample of stars with higher membership probability, by selecting all the objects within  $3\sigma$  from the MS-SGB-RGB line (where  $\sigma$  represents the mean error in color as a function of magnitude, as calculated from the artificial star experiments, and the fiducial line has been drawn by hand). BSS, HB and photometric blends (see previous discussion) were added to this sample.

Artificial star tests have been performed in order to investigate the completeness of our sample. A total of  $\sim 60,000$  stars have been added in 40 separate runs. The results of these experiments show that the 50% completeness level is located at  $V \simeq 22.5$  and  $I \simeq 21.5$ . Only the stars above these limits (marked by a dashed line in Fig. 3) have been selected for the following analysis. In order to get a meaningful profile it is also critical that no radial de-

pendence of the completeness exists. We checked that the completeness profile is constant in the range  $R \geq 20$  arcsec from the cluster center, while a slight rise in magnitude of the 50% level is observed in the inner region.

The star subsample defined with the previous criteria is identified by filled circles in Fig. 3, whereas open circles mark probable halo field stars. The same convention is used in the maps presented in Fig. 1.

In order to compare the Pal 12 CMD with other clusters and theoretical isochrones, a discussion of its relevant parameters is now given.

### 3.1. Metallicity

A summary of early studies on Pal 12 metallicity is presented in S89. Although a large uncertainty in the metal content determinations for Pal 12 existed at the time, a combination of several metallicity indices yielded a value comprised between the ones of M5 and 47 Tuc (i.e.  $[\text{Fe}/\text{H}] = -1.0 \pm 0.3$ ).

Since then, three new metallicity determinations have been obtained: besides new CCD photometry, low and high resolution spectra have been analyzed for a few giant stars. These stars are marked with open squares both in the cluster's map (Fig. 1, right panel) and in the CMD (Fig. 3, left panel).

Da Costa & Armandroff (1990) derived  $[\text{Fe}/\text{H}] = -1.06 \pm 0.12$  from  $V, I$  photometry of 20 Pal 12 giant branch stars, by comparing the position of the RGB with other calibration clusters. Applying the same method to our data, we obtain a value  $[\text{Fe}/\text{H}] \simeq -0.93$ , where the small difference, well within the uncertainties, is mainly due to our 0.06 mag redder colors (see Sect. 2).

Armandroff & Da Costa (1991, DA91) obtained the metallicity from the Ca II triplet strengths, and found  $[\text{Fe}/\text{H}] = -0.60 \pm 0.14$  for Pal 12, later confirmed by Da Costa & Armandroff (1995;  $[\text{Fe}/\text{H}] = -0.64 \pm 0.09$ ).

The most recent result has been obtained by Brown et al. (1997). They present high-resolution spectra of the two brightest stars of AD91, obtaining a  $[\text{Fe}/\text{H}] = -1.0 \pm 0.1$ . They also analyzed the  $[\alpha/\text{Fe}]$  abundances, obtaining a zero value.

In view of the larger uncertainties related to indirect metallicity determinations with respect to high resolution spectroscopy, in the following we will adopt  $[\text{Fe}/\text{H}] = -1.0$  for Pal 12, and assume a null  $\alpha$  element enhancement.

### 3.2. Reddening

The interstellar reddening towards Pal 12 is expected to be low, given the high galactic latitude of the cluster. Although no accurate estimates exist, two independent values have been suggested; HC80 adopted a value of  $E(B - V) = 0.02 \pm 0.02$  from the cosecant law (Harris

& Racine 1979), and noted that this value is consistent with that estimated from the color-color diagram of stars in their photoelectric sequence,  $E(B - V) < 0.03$ . A small reddening is also indicated by the maps by Burstein and Heiles (1982):  $0.00 < E(B - V) < 0.03$ . Adopting  $E(V - I) = 1.28 E(B - V)$  (Dean et al. 1978), we obtain the value  $E(V - I) = 0.03 \pm 0.02$ , which will be the assumed reddening throughout this paper.

### 3.3. Distance

Distance moduli of the Palomar class clusters have been often overestimated in the past. Kinman & Rosino (1962) searched Palomar 12 for variables. They found three variables, one of them previously discovered by Zwicky (1957). Based on the mean apparent magnitude of these RR Lyrae, Pal 12 was initially located farther than 50 kpc from the Galactic center (Harris 1976). It is only after HC80 photometric study that a more precise distance modulus has been given (about 14 kpc), on the basis of the  $V$  magnitude of the poorly populated HB.

We derive the distance to Pal 12 by comparing its HB with that of NGC 6362, which is the only GC at  $[\text{Fe}/\text{H}] \simeq -1$  with measured  $\alpha$ -elements abundance (cf. Tab. 2 in Carney, 1996). Piotto et al. (1998) give  $M_V(\text{HB}) = 0.78 \pm 0.05$  for NGC 6362; this value is *not* representative of the Pal 12 HB luminosity, since we must correct for the age (cf. Sect. 4) and  $\alpha$  abundance offsets between both clusters.

A decrease in age implies an increase in the HB stars mass and luminosity, the exact dependency being a function of  $Z$ . Although no  $Z = 0.002$  (the Pal 12 metallicity) models are available, an interpolation from the  $Z = 0.001$  and  $Z = 0.004$ , Bertelli et al. (1994, hereafter B94) model isochrones leads to estimate a change  $\Delta M_V \sim -0.07$  mag, which reduces the age by 30% (cf. Sect. 4).

Spectroscopy of 2 NGC 6362 giants has been obtained by Gratton (1987), who measured  $[\alpha/\text{Fe}] = 0.32 \pm 0.09$ . In view of the results by Brown et al. (1997) presented in Sec. 3.1, a comparison of the Pal 12 CMD with NGC 6362 must take into account the “ $\alpha$ -enhancement” of the latter.

As discussed in more detail in Sect. 4, an increase of 0.3 dex in  $[\alpha/\text{Fe}]$  mimics an increase of 0.2 dex in the equivalent  $[\text{Fe}/\text{H}]$ , and implies a decrease in the HB brightness. The exact value depends on the slope of the luminosity-metallicity relation for the HB. Although this is still controversial, a typical value  $\Delta M_V / \Delta[\text{Fe}/\text{H}] = 0.20$  can be used (Carney et al. 1992), which therefore means  $\Delta M_V = 0.04$  mag in our case.

We should also take into account possible differences in the mass loss rates along the RGB between the two clusters. These would affect the ZAHB mass, and hence its luminosity. In order to constrain such an effect, we can compare the colors of the red HB of Pal 12 and NGC 6362. Indeed, using again the B94 isochrones we find that, in the

red HB region, a change in the ZAHB mass of  $+0.1M_\odot$  will change the HB location of a star by  $+0.22$  mag in  $(B - V)$  and  $-0.07$  mag in  $V$ . The effect is therefore three times larger in the  $(B - V)$  color than in the  $V$  magnitude.

The actual dereddened colors of the red HBs of the two clusters are  $(B - V)_0 \sim 0.73$  for Pal 12 (Stetson et al. 1989), and  $(B - V)_0 \sim 0.54$  for NGC 6362 (Piotto et al. 1998). Hence, a color difference of  $\sim 0.2$  mag in  $(B - V)$  exists between Pal 12 and NGC 6362, which corresponds to a  $< 0.1M_\odot$  mass loss difference.

However, this higher HB mass for Pal 12 is consistent with its lower age. According to B94, the turnoff mass of a cluster will change by  $\sim 0.1M_\odot$  if its age is changed by  $\sim 5$  Gyr. Since, in the B94 scale, the typical GC age would be  $t \sim 14 \div 15$  Gyr (Saviane et al. 1998), the higher mass of the Pal 12 HB is easily explained by its  $\sim 30\%$  lower age (cf. Sect. 4). A mass loss differential correction is therefore not needed.

In summary, we expect that the Pal 12 HB should be 0.07 mag brighter than that of NGC 6362 in view of its younger age and 0.04 mag brighter due to its lower  $\alpha$  element content, i.e.  $M_V(\text{HB}) = 0.67 \pm 0.05$ .

As the apparent magnitude of the Pal 12 HB is  $V_{\text{HB}} = 17.18 \pm 0.02$  (where the error has been computed taking into account the calibration uncertainties), the apparent distance modulus becomes  $m - M_V = 16.51$ . Given the assumed reddening  $E(B - V) = 0.02$ , the absolute distance modulus is  $(m - M)_0 = 16.45 \pm 0.10$ . The estimate of the error includes the uncertainties on the calibration zero-point, on the magnitude of the NGC 6362 HB, and on the absorption. Our value of the distance to Pal 12 is perfectly compatible with previous estimates: HC80 give  $16.2 \pm 0.35$ , GO88  $16.1 \div 16.5$ , S89  $16.3$ , and DA90  $16.46$  for the absolute distance modulus.

The adopted distance modulus corresponds to a distance from the Sun  $R_\odot = 19.5 \pm 0.9$  Kpc, a distance from the Galactic center  $R_{GC} = 16.2 \pm 0.7$  kpc, and a height  $Z_{GP} = 14.4 \pm 0.7$  below the Galactic plane (we adopted a distance from the Sun to the Galactic center  $R = 8.0 \pm 0.5$  kpc; Reid 1993).

## 4. Age

The first evidence of a relatively young age for Pal 12 was given by GO88, who estimated that Pal 12 must be 30% younger than 47 Tuc on the basis of an atypically small value of the magnitude difference between the HB and the TO. Indeed, this was the first clear identification of a young GGC.

Almost at the same time, S89 presented an independent  $BV$  CCD study. They compared the Pal 12 fiducial RGB to those of 47 Tuc and M5, which bracket Pal 12 metallicity, concluding that no match could be found. The simplest explanation was that Pal 12 is younger than the other two clusters by some 25%-30%.

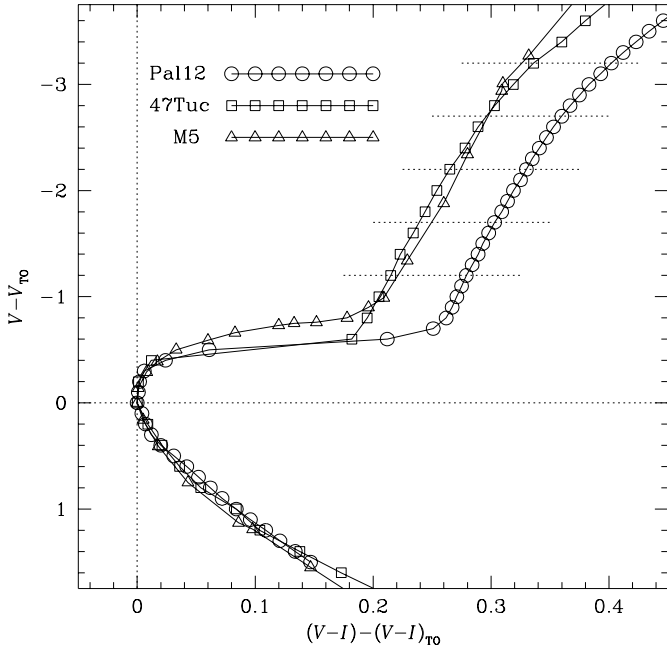


**Fig. 5.** The fiducial points for M5, 47 Tuc and Pal 12 are presented, after that the TOs have been shifted in magnitude and colors to a common value. A large difference in color exists between the RGBs of the two template clusters and the Pal 12 RGB. The small color difference between the RGB of M5 and the one of 47 Tuc (whose metallicities encompass that of Pal 12) demonstrates that a 0.5 dex difference in metallicity has small influence on the  $V - I$  color-difference between the RGB and the TO. Pal 12 must therefore be younger than the two template clusters.

In both studies, the 47 Tuc fiducial lines were taken from Hesser et al. (1987, hereafter H87). These fiducials were constructed by merging  $B$  and  $V$  CCD photometry for 8800 stars below the MS turnoff to the evolved part of the CMD coming from earlier photographic work (Hesser & Hatwick 1977, Lee 1977). Also the HB and MS fiducial lines of M5 come from two different studies (*cf.* S89 for more details). Possible photometric calibration discrepancies between the different datasets contribute to the age uncertainty in these early estimates.

The heterogeneity of the data base for the comparison clusters and the high uncertainty in the metal content do not allow us to quantify the error associated to the results by GO88 and S89. In the following we will attempt a new, independent determination of the Pal 12 *relative* age by comparison with suitable template clusters.

Since no GGCs with metallicity  $[\text{Fe}/\text{H}] \sim -1.0$  have been observed to date in the  $V, I$  bands, as done by the previous authors, we will use 47 Tuc (NGC 104) and M5 (NGC 5904), whose metallicities bracket that of Pal 12. These are the nearest metallicity clusters for which (a) published homogeneous  $V, I$  photometry exists, from the RGB tip down to the MS; (b) both  $[\text{Fe}/\text{H}]$  and  $\alpha$ -elements

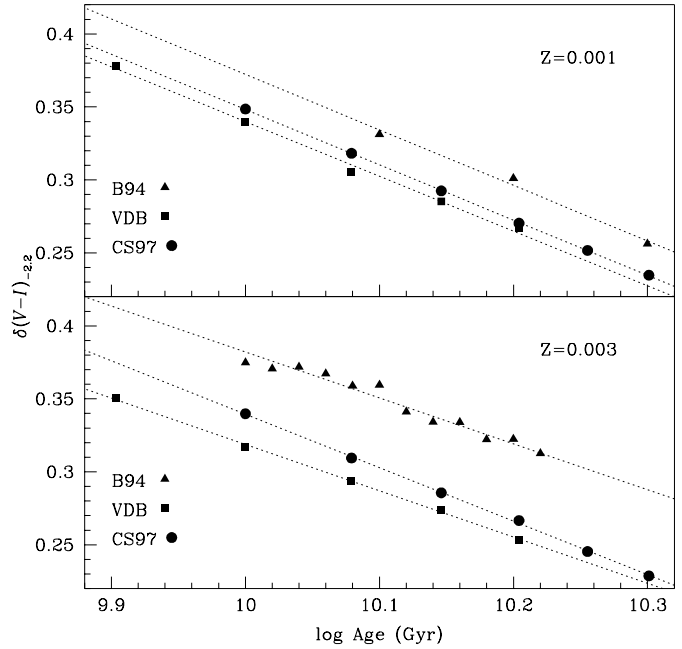


**Fig. 6.** RGB-TO ( $V - I$ ) color-differences at 2.2 mag above the TO have been computed using B94, V98, and S97 isochrones, for different ages and for the two labeled metallicities. Keeping the metallicity fixed, a linear relation with the same slope (within  $\pm 1\%$ ) is found between the RGB-TO color width and the logarithm of age, regardless of the model used. The discrepant zero-points are partly due to different assumptions on the  $\alpha$ -element content of the three theoretical sets. The similarity in the slope shows that the three sets of models give consistent relative ages, at least in the small metallicity interval considered here.

abundance have been obtained from high-resolution spectroscopy; (c) do not show any age anomaly either in published or in our preliminary analysis of GGC relative ages.

The best  $VI$ , photometric sample for 47 Tuc is that of Kaluzny et al. (1998, see Paper I for a discussion of the other available  $VI$  CMDs for 47 Tuc). Two photometric catalogs can be used for M5, namely Sandquist et al. (1996) and Johnson & Bolte (1998). Since Johnson & Bolte discuss possible problems in their earlier calibrations of the M5 photometry, we will use the most recent sample. In any case, the stellar  $V - I$  colors are the same in the two studies.

The metallicities and  $\alpha$  abundance ratios have been taken from Tab. 2 of Carney (1996):  $[\text{Fe}/\text{H}] = -0.73$  and  $[\alpha/\text{Fe}] = 0.18 \pm 0.03$  for 47 Tuc, and  $[\text{Fe}/\text{H}] = -1.22$  and  $[\alpha/\text{Fe}] = 0.30 \pm 0.03$  for M5.

Figure 5 shows the fiducial points of M5, 47 Tuc and Pal 12 registered to a common TO point. It is clear that, while the RGBs of 47 Tuc and M5 are almost overlapping, the RGB of Pal 12 is significantly redder. The modest color shift between the RGB of M5 and that of 47 Tuc shows that metallicity differences have small influence on

the RGB–TO color-difference, in the  $V$  vs.  $V - I$  plane. A change of 0.5 dex in metallicity implies a color offset as small as 0.01 mag. This fact is confirmed by the theoretical models, and has been pointed out by Saviane et al. (1997). Assuming an age of 14 Gyr, the models of Vandenberg 1998 (hereafter V98) predict a change of 0.011 mag in  $\delta(V - I)$  increasing the metallicity from  $Z = 0.002$  to  $Z = 0.003$  (the color difference between the RGB and the TO has been measured at 2.2 mag above the TO).

The position of the Pal 12 RGB cannot therefore be explained by a simple metallicity effect. The observed difference in the location of the RGB of Pal 12 with respect to 47 Tuc and M5 must be due either to a different  $\alpha$  element abundance or to an age effect.

We begin by examining the first possibility. According to Salaris et al. (1993), an enhancement by a factor  $f$  in the ratio  $X_\alpha/X_{\text{Fe}}$  is equivalent to an increase of a factor  $(0.638f + 0.362)$  in the metallicity  $Z$ . As discussed in Sec. 3.1, the current measurements give  $[\alpha/\text{Fe}] = 0, 0.2$  and  $0.3$  for Pal 12, 47 Tuc and M5, respectively. This means that, in order to compare the Pal 12 fiducials with the reference clusters, we must take into account these differences in  $\alpha$  element abundances, which correspond to increasing the Pal 12 metallicity by  $\sim 0.2$  dex. The  $\alpha$ -enhancement effect makes the  $[\text{m}/\text{H}]$  of Pal 12 close to that of 47 Tuc. Therefore, Fig. 5 shows that the  $\alpha$  element abundance differences cannot justify the large observed RGB color differences.

An age difference is the only remaining explanation. In order to make an estimate of the Pal 12 relative age, we have measured  $\delta(V - I)$  between the TO and the RGB for different (fixed)  $V - V_{\text{TO}}$  values in the models of B94, Straniero et al. (1997, hereafter S97), and Vandenberg (1998, hereafter V98). The first two sets of models are *non- $\alpha$ -enhanced*, while the third one is. Figure 6 displays the  $\delta(V - I)$  for  $V - V_{\text{TO}} = -2.2$  mag as a function of the logarithm of age. With a good approximation,  $\delta(V - I)$  linearly depends on the logarithm of age. The  $-2.2$  mag level has been chosen after an analysis of the behavior of the TO–RGB color difference with respect to the age. We have repeated our measurements at the RGB levels marked by dotted lines in Fig. 5 and found that, if a value  $V - V_{\text{TO}} > -1.2$  is taken, the SGB plays an important role, making relative measurements difficult to interpret. The same occurs for  $V - V_{\text{TO}} < -3.5$ , where the slope of the RGB becomes very sensitive to the clusters metallicity. Conversely, for  $V - V_{\text{TO}}$  in the range  $[-1.2 \div -3.2]$  and age older than 8 Gyrs, the  $\delta(V - I)$  seems to be almost independent of metallicity. We simply chose a mean value  $-2.2$ . The linear relations in Fig. 5 have the same slopes for  $Z = 0.001$ , while for  $Z = 0.003$  the B94 and V98 models give the same slope, which is slightly different from that obtained from S97. The zero points are different, but this does not affect the relative age determination. We will therefore obtain the same relative ages when using either the B94, V98 or S97 models at  $Z = 0.001$ , while the S97

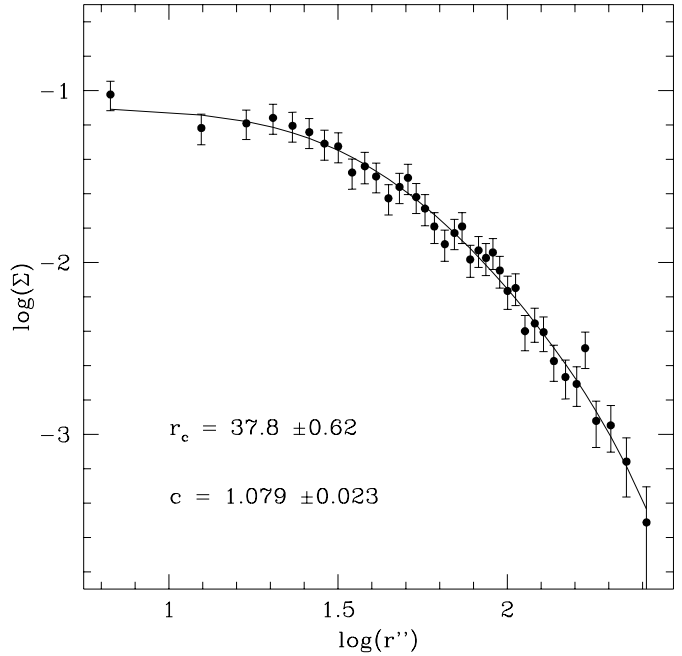


**Fig. 7.** Profile determination for Palomar 12; filled circles represent the observed star counts and the solid line the best-fitting King law. The adopted morphological parameters are  $r_c = 37.8 \pm 0.6$  and  $c = 1.08 \pm 0.02$ .

isochrones give age differences larger by  $\sim 4\%$  than B94 or V98 at  $Z=0.003$ .

From Fig. 5 we have  $\delta(V - I)=0.280$  for M5,  $\delta(V - I)=0.265$  for 47 Tuc, and  $\delta(V - I)=0.330$  for Pal 12. Assuming  $Z=0.003$ , from Fig. 6, we obtain that Pal 12 is 34%, 34%, or 30% younger than 47 Tuc on the basis of V98, B94 and S97 models, respectively. As discussed above, adopting  $Z=0.001$  we have quite similar results: formally, Pal 12 is 33%, 32%, or 32% younger than M5. Taking into account the errors in measuring the  $\delta(V - I)$  parameter (estimated assuming an uncertainty of  $\pm 0.15$  mag and  $\pm 0.01$  mag in the magnitude and color of the TO) for both Pal 12 and the reference clusters, the uncertainties in the relative ages is of the order of 10%. We conclude that Pal 12 has an age  $68\% \pm 10\%$  that of a typical GGC, assuming that 47 Tuc and M5 age are representative of the ages of the bulk of the GGC population (Buonanno et al 1998).

## 5. Structural Parameters

We have derived the density profile of Pal 12 making radial star counts in equal number-of-stars steps. Stars with high membership probability were selected as explained in Sect. 3. The cluster center was determined in an iterative manner, by first computing a median of the  $x$  and  $y$  coordinates of the stars within an arbitrarily located circle of radius  $r = 160''$ . Next, a new circle was considered with its center corresponding to the just obtained median point. The process was repeated until two subsequently computed centers were coincident. The offset between our



center and that given by HC80 is just  $3''$  in RA and  $-5''$  in DEC. The background level was estimated outside a suitably large distance from the cluster center, chosen with the following procedure. First, a King law was fitted to the observed profile, and a set of structural parameters was derived. Then the procedure was repeated until the computed tidal radius was smaller than the radius used for the foreground estimate.

The final result is shown in Fig. 7, where the filled circles represent the observed star counts and the solid line the best-fitting King law. The adopted morphological parameters are  $r_c = 37.8 \pm 0.6$  and  $c = 1.08 \pm 0.02$ , where the errors were estimated following the methods adopted by Saviane et al. (1996), and represent the formal uncertainties of the fit.

A more reliable estimate of the errors was computed by keeping the central density fixed and varying the other 2 parameters in a grid of values. The 90% confidence ranges of the fit for the tidal radius and concentration are  $r_c = 37.8^{+3.30}_{-5.16}$  and  $c = 1.08^{+0.33}_{-0.08}$ . An alternative estimate of the uncertainties of the parameters was obtained by changing the sky level by  $\pm 3\sigma$ . The effect is to lower  $r_c$  by  $\sim 1.5''$  and to change  $c$  by  $\sim \pm 0.1$ .

Our structural parameters are significantly different from those published in Trager et al. (1995); the authors quote  $\log r_c = 0''.23$  and  $c = 1.94$ , which imply a tidal radius  $r_t = 2''.46$ . Since stars belonging to Pal 12 are clearly seen beyond this radial limit (cf. Fig. 3), it is clear that the Trager's et al. tidal radius is too small. On the other hand, the same authors had previously listed values closer to ours (Trager et al. 1993), analyzing the same data used by Trager et al. (1995). It is therefore possible that the inconsistency comes from some typo in Trager et al. (1995) table.

As a final remark, we notice that a dip in the profile is observed in the very central region. This could be due to a slightly lower completeness as discussed in Sect. 3. We fitted the profile also removing the central 3 points, obtaining almost identical structural parameters.

## 6. Summary and conclusions

The first deep  $V$ ,  $I$  CCD photometry for the Galactic globular cluster Palomar 12 has been presented. The wide field allowed us to sample the cluster stellar population well beyond the tidal radius. All stars in our field down to  $\sim 2$  mag below the MS turnoff (50% completeness level) have been measured, allowing a clear definition of all the CMD sequences.

Using the HB brightness, an improved distance determination has been obtained by comparison with NGC 6362 as a reference cluster.

A direct comparison with homogeneous  $V$ ,  $I$  CMDs for 47 Tuc and M5 shows that Pal 12 is a young cluster. The computation of a precise relative age depends on the theoretical isochrones used, although differences of at most

4% are found among the three models considered (B94, V98 and S97). The comparison with the models shows that Pal 12 age is  $68\% \pm 10\%$  that of the reference clusters.

Finally, our large field also allowed to obtain a radially complete number density profile for stars brighter than  $V = 22.5$ , and to compute improved structural parameters. The new morphological parameters are  $r_c = 37.8 \pm 0.6$  and  $c = 1.08 \pm 0.02$ .

## References

- Armandroff, T.E., Da Costa, G.S., 1991, AJ 101, 1329 (AD91)  
 Bertelli, G., Bressan, A., Chiosi, C., Fagotto, F., Nasi, E., 1994, A&ASS 106, 275 (B94)  
 Brown, J.A., Wallerstein, G., Zucker, D., 1997, AJ 114, 180  
 Buonanno, R., Buscema, G., Fusi Pecci, F., Richer, H.B., Fahlman, G.G., 1990, AJ 104, 1811  
 Buonanno, R., Corsi, C.E., Fusi Pecci, F., Richer H.B., 1995, AJ 109, 650  
 Buonanno, R., Corsi, C.E., Pulone, L., Fusi Pecci, Bellazzini, M., 1998, A&A 333, 505  
 Buonanno, R., Corsi, C.E., Pulone, L., Fusi Pecci, F., Richer, H.B., Fahlman, G.G., 1995, AJ 109, 663  
 Burstein, D., Heiles, C., 1982, AJ 87, 1165  
 Carney, B.W., 1996, PASP 108, 900  
 Carney, B.W., Storm, J., Jones, R.W., 1992, ApJ 386, 663  
 Cheboyer, B., Demarque, P., Sarajedini, A., 1996, ApJ 459, 558  
 Da Costa, G.S., Armandroff, T.E., 1990, AJ 101, 1329 (DA90)  
 Da Costa, G.S., Armandroff, T.E., 1995, AJ 109, 2533  
 Dean, J.F., Warner, P.R., Cousins, A.W.J., 1978, MNRAS 183, 569  
 Gratton, R.G., 1987, A&A, 179, 181  
 Gratton, R.G., Ortolani, S., 1988, A&AS 73, 137 (GO88)  
 Grillmair, C.J., Freeman, K.C., Irwin, M., Quinn, P.J., 1995, AJ 109, 2553  
 Harrington, Zwicky F., 1953, In: *Ann. Rpt., Mt. W. and Palomar Obs.*, 1953-54, 23  
 Harris, W.E., 1976, AJ 81, 1095  
 Harris, W.E., 1996, AJ 112, 1487  
 Harris, W.E., Canterna, R., 1980, ApJ 239, 815 (HC80)  
 Harris W.E., Racine R., 1979, ARA&A 17,241  
 Hesser, J.E., Harris, W.E., Vandenberg, D.A., Allwright, J.W.B., Shott, P., Stetson, P.B., 1987, PASP 99, 739  
 Hesser, J.E., Hartwick, F.D.A., 1977, ApJS 33, 361  
 Johnson J.A., Bolte M., 1998, AJ 115, 693  
 Kaluzny, J., Kubiak, M., Szimanski M., UDalski A., Krzemiński W., Mateo M., Stanek K.Z., 1998, A&AS 128, 19  
 Kinman, T.D., Rosino, L., 1962, PASP 74, 499  
 Landolt, A.U., 1992, AJ 104, 340  
 Lee, S.W., 1977, A&ASS 27, 381  
 Piotto, G., Zoccali, M., King, I.R., Djorgovski, S., Sosin, C., Dorman, B., Rich, M., 1998, AJ, submitted  
 Reid, M.J., 1993, ARA&A 31, 345  
 Rosenberg, A., Saviane, I., Piotto, G., Aparicio, A., Zaggia, S., 1998, AJ 115, 648 (Paper I)  
 Salaris, M., Chieffi, A., Straniero, O., 1993, ApJ, 414, 580  
 Sandquist, E.L., Bolte, M., Stetson, P.B., 1996, ApJ 470, 910  
 Saviane I., Held E.V., Piotto G., 1996, A&A, 315, 40  
 Saviane, I., Held, E.V., 1998, A&A, submitted (SH98)

- Saviane, I., Rosenberg, A., Piotto, G., 1997, In: *Advances in Stellar Evolution*, ed. R. T. Rood & A. Renzini (Cambridge: Cambridge U. Press), p. 65
- Saviane I., Piotto G., Fagotto F., Zaggia S., Capaccioli M., Aparicio A., 1998, *A&A*, 333, 479
- Stetson, P.B., 1987, *PASP* 99, 191
- Stetson, P.B., Vandenberg, D.A., Bolte, M., Hesser, J.E., Smith, G.H., 1989 *AJ* 97,1360 (S89)
- Stetson, P.B., Vandenberg, D.A., Bolte, M., 1996, *PASP* 108, 560
- Straniero, O., Chieffi, A., Limongi, M., 1997, *ApJ* 490, 425
- Trager, S.C., King, I.R., Djorgovski, S., King, I.R., 1993, *PASPC* 50, 347
- Trager, S.C., King, I.R., Djorgovski, S., 1995, *AJ* 109, 218
- Vandenberg, D., 1998, (priv. comm) V98
- Zaggia, S., Piotto, G., Capaccioli, M., 1997, *A&A* 327, 1004
- Zwicky, F., *Morphological Astronomy* (Berlin: Springer, 1957) 205